Chapter 9
Ferrous Material Fill: Magnetization Channels, Layer-by-Layer and Average Permeability, Element-to-Element Field

Anna A. Sandulyak, Darya A. Sandulyak, Vera A. Ershova, and Alexander V. Sandulyak

Abstract For the magnetic samples of heterogeneous (including bulk) ferrous-materials, a qualitative, and according to the data on the demagnetization factor N of finely dispersed samples quantitative assessment of the volume fraction is provided for the characteristic intervals γ of the ferrous component. There are three intervals: the first one is $\gamma \leq 0.2$, the second one is $0.2 < \gamma \leq 0.4 - 0.45$, and the third one is $\gamma > 0.4 - 0.45$ (up to $\gamma \cong 0.6$ for a material filled with "densely packed" granules or grains). It should be noted that samples of heterogeneous ferrous materials within the third interval γ, according to the stabilization of N and its proximity to the N-value for a uniform sample (which indicates a "magnetic splicing" of the ferroelements in the heterogenous material), possess the features of a uniform magnetic sample and, therefore, they fully correspond to the notion of a quasi-uniform object. Special attention is paid to filling of granules or grains (with their inherently stable value of γ) as a completely independent class of heterogeneous ferrous materials.

In order to solve the actual problems related to the determination of magnetic properties for the filling of ferroelements (granules, grains), it is preferable to use the model of selective, channeled magnetization. At the same time, the concept of this model implies obtaining necessary theoretical and experimental solutions both for the channel as a whole and for its parts (conditional cores and tube layers of different radius). In addition, such key parameters of the model as magnetic permeability of channel tube layers $\tilde{\mu}$ and their cores $< \tilde{\mu} >$ (averaged data of $\tilde{\mu}$) depending on their radius and intensity of magnetization field will be analyzed. It is shown the compliance of experimental data with theoretical data. The physical meaning of the parameter $\tilde{\mu}$ reveals: it corresponds to the relative field strength h in the pores between granules.

Anna A. Sandulyak · Darya A. Sandulyak · Vera A. Ershova · Alexander V. Sandulyak
Moscow Technological University, Moscow, Stromynka 20, Russia,
e-mail: anna.sandulyak@mail.ru, d.sandulyak@mail.ru, v.ershova@mail.ru
e-mail: a.sandulyak@mail.ru

H. Altenbach et al. (eds.), *Analysis and Modelling of Advanced Structures and Smart Systems*, Advanced Structured Materials 81,
https://doi.org/10.1007/978-981-10-6895-9_9

9.1 Introduction. Qualitative Assessment of Typical Intervals for the Volume Fraction of a Ferrous Component

Progressive multi-purpose use of various heterogeneous ferrous materials (dispersed, with a ferrous magnetic component) (Ravnik and Hriberšek, 2013; Nielsch et al, 2002; Lacoste and Lubensky, 2001; Diguet et al, 2010; Anhalt et al, 2008; Anhalt and Weidenfeller, 2007; Schulz et al, 2010; Bottauscio et al, 2009), including solid composite and bulk (granular, acinose, powder) materials, magnetic suspensions and colloids, requires the solution of a number of physical problems. One of those problems is the determination of the averaged magnetic properties of these materials, for example, averaged (per volume) magnetic permeability and susceptibility (Ravnik and Hriberšek, 2013; Nielsch et al, 2002; Diguet et al, 2010; Anhalt et al, 2008; Anhalt and Weidenfeller, 2007; Ngo and Pileni, 2001; Schulz et al, 2010; Hultgren et al, 2005; Daniel and Corcolle, 2007; Bottauscio et al, 2009). Furthermore, the problem of obtaining information on the field between the elements of a ferrous magnetic material (in particular, between mutually contacting ferrous granules) is also in high demand, especially for magnetophoresis when magnetizable granular fill media are used as filter matrices of magnetic separators, analyzers of filter matrices of magnetic separators and analyzers of ferroimpurities disperse phase of various media (Sandulyak et al, 2015c, 2017a,c).

From the standpoint of these problems, the issue of universal modeling of such ferrous materials and their magnetization with obtaining theoretical and experimental solutions, which simultaneously cover the entire range of volume concentration of the ferrous magnetic component γ, i.e. within $0 \le \gamma \le 1$, is recognized as complex, and hardly solvable. This is due to specific features of ferrous material magnetization at those or other values of γ, i.e. at any mutual distancing of elements in the ferrous magnetic component (what determines the degree of mutual magnetic influence for the ferroelements).

More preferable is to make separately the task definition and solution of specified problems for the certain characteristic γ intervals. Based on the existing concepts, there should be three basic γ intervals that are different in their roles. The two of these are the intervals below and above the critical, percolation transition between the states of so-called "giant magnetoresistance" and "total" metallic conductivity. Another one interval corresponds to this very (not abrupt) transition. In this case, the "giant magnetoresistance" (we should note that this term is not traditional concept of conventional magnetic resistance but high electrical resistance of a heterogenous ferrous material sample in a magnetic field exposure) is inherent, of course, to samples with relatively low γ-values, i.e. with guaranteed mutual separation of ferroelements in it. And the state of metallic conductivity is caused by the occurrence and further increase (with increasing γ) in the number of direct contacts between the ferrous elements, the emergence and increase in the number of "through target" chains of ferrous granules and ensembles of such chains, up to the limit (inherent in filling) coordination number of ferroelements.

9.2 Quantitative Assessment of Characteristic Intervals for the Volume Fraction of a Ferrous Component and its Values for the Filling Materials

Convincing concretization of three characteristic intervals for the volume fraction of ferrous component γ, mainly quantitative, directly follows from the results of the determination of demagnetization factor N for a fine-grained material sample (ferrous particles sizes are 3-100 μm Mattei and Floc'h, 2003). Thus, this factor, as an inherent property of any magnetic sample of certain sizes and shapes, can serve as a kind of indicator for the mutual magnetic influence of ferroelements during magnetizing the sample of a heterogenous ferromaterial.

The results (Mattei and Floc'h, 2003) indeed indicate the three typical intervals of γ, which are given below. The first: $\gamma \leq 0.2$, where $N = 0$. The second: $0.2 < \gamma \leq 0.4 - 0.45$, where N is a variable increasing from zero to a certain value. The third: $\gamma > 0.4 - 0.45$ (and up to the limit value for granular or grained filling medium: $\gamma \cong 0.6$), here N maintains a stable N-value which is achieved at the end of the previous γ interval.

Let us give some comments to these statements.

- In the first interval with $\gamma \leq 0.2$ the ferroelements are clearly at a significant mutual distance within the sample: for the ferroelements of conventionally spherical shape $(\pi/6\gamma)^{1/3} = 1.4$ and more times greater than their own size. As a consequence, they are magnetized fully autonomously, practically without affecting magnetic influence on each other - with the demagnetizing factor inherent to each individual ferroelement (rather than the sample as a whole). The absence of such an influence caused by the segregation of ferroelements does not give reasons to speak here that such a sample is a magnetic body (due to the absence of N which means the lack of features for this). In this case it is just a sample representing a "set" of individual, spatially and functionally scattered ferroelements.
- In the second interval with $0.2 < \gamma \leq 0.4 - 0.45$ (characterized by mutual approach of ferroelements, by appearing of contacts with each other), mutual magnetic influence already manifests itself judging by the fact that here $N \neq 0$. With increasing γ it is amplified and since in this interval the value of N is not yet stable (varies), we can speak here only that one gets a sample formation as a magnetic body.
- In the third interval with $\gamma > 0.4 - 0.45$ (characterized by forming a plurality of mutual contacts between the ferroelements until reaching a maximum possible coordination number here), the mutual magnetic influence becomes so significant that, in fact, "magnetic splicing" of ferroelements takes place in the sample. In this case, it is quite possible to speak already about the fact of magnetic body formation. Such a sample according to N = const acquires properties of a uniform magnetic body (a body of a certain shape, for example, cylindrical - with a certain ratio of length to diameter). Moreover, in studies (Mattei and Floc'h, 2003) with a fine-grained sample of cylindrical shape (length $l = 2$ cm and diameter $d = 0.4$ cm, hence: $l/d = 5$) the obtained values of $N = 0.058 - 0.066$ were comparable with

the values of $N = 0.04 - 0.05$ for a uniform sample of the same relative dimensions l/d (Sandulyak et al, 2015a). Such a sample can also be described as a kind of "uniform" (more accurately - quasi-uniform) sample. In this third interval there are the so-called "densely packed" (formed during filling into a container) granular or grained media, constituting a rather extensive class of industrial purpose media.

The structures of granular (grained), in particular, classical poly-spherical media lend themselves to modeling, especially for known versions of their artificial ordering. At the same time, basic parameters of such structures are determined in the most rational way, for example, packing density, porosity, co-ordination number, equivalent diameter of pores, their tortuosity, etc., only on the basis of a model with fractional (allowing the presence of conditionally fractional parts of pellet balls) cells of such structures (Sandulyak et al, 2008, 2016a,b, 2017b,d). These are the quasi-bound parallelepiped cells with vertices at the centers of eight neighboring pellet balls which completely satisfy the principle of the structure block layout as a whole. Thus, for example, the model provides quite expected (in accordance with other models) values of the volume fraction γ of spheres: from $\gamma \cong 0.52$ for the simplest cubic packing of spheres to $\gamma = 0.74$ for the packing of spheres with a more complex geometry of their relative position. Hence, the interval of possible γ variation for the granular (grained) packages, even for artificially ordered ones, is relatively small.

As for the actual and widely used filling of granules (grains), γ interval for them is further narrowed and it actually equals $\gamma = 0.55 - 0.64$ (Sandulyak et al, 2008, 2016a,b, 2017b,d; Bennacer et al, 2013; Zhang and M., 2003; Kim and Whittle, 2006). And within this narrowed γ interval the value of γ has only a weak dependence on the overall dimensions (diameter D) of the container, where the pellet balls with a diameter d - ranged as $D/d = 4 - 30$ are filled (Sandulyak et al, 2016b, 2017b). For a specific value of D/d the said γ interval, essentially, ceases to be such, and it is degenerated into one or another particular γ-value. In this case, according to the obtained γ values (average $\gamma \cong 0.6$), there is an objective reason to consider the filling of granules (grains) close to one of the ordered granules, not the most dense packing of spheres - with a simple chess-corridor order of their mutual arrangement (Sandulyak et al, 2008, 2016a,b, 2017b,d).

9.3 Selective (in the Form of Chains of Channels) Magnetization of Ferrous Material. Concept of Layer-Tube Channels

In order to solve the above-stated problems with respect to the ferrous material in the form of filling granules or grains ("densely packed", contacting each other), it is expedient to use the model of channeled magnetization of this ferrous material. In Sandulyak (1983, 1982, 1984) it was shown that granular ferrous material, in particular, the poly-ball medium is magnetized in a selective manner through efficient "elementary" channels in accordance with magnetization direction. Among the set of granules-links of the branched skeletal structure of the granular medium there are

always real straight or sinuous chains of granules corresponding to this direction. In other words, such a medium is a kind of bundle of effective "elementary" channels that penetrate the fill medium along magnetization direction.

The development of such a model is the concept in Sandulyak (1983, 1984); Sandulyak et al (2009, 2007, 2010), according to which the effective elementary channels of magnetization are not equivalent in cross-section but have a definite magnetization profile (by analogy with the profile of the fluid flow rate in a pipe). So, this channel (conducting magnetic flux), although it can in principle be characterized by averaged values of magnetic induction and permeability (Sandulyak, 1982). Nevertheless, in the cross-section significant differences in the values of these parameters can be observed.

In other words, if the effective channel is conventionally represented in the form of concentric layer-tubes, then as the radius increases, the ability to conduct the magnetic flux decreases. This is due to the fact that the magnetic resistance of each of these artificially isolated, quasi-uniform tubular layers of the channel's cross section (Fig. 9.1) is clearly not the same[1] (Sandulyak, 1983; Sandulyak et al, 2009). Thus, as the radius of the "incremental" tubular layer increases, its magnetic resistance increases due to the increasing distance between the surfaces of adjacent granules-links (Fig. 9.1). As a consequence, the average magnetic permeability of the layer-tubes (and induction in them) decreases, and, therefore, their ability to conduct magnetic flux decreases.

Suppose that one thin tube (Fig. 9.1a) of arbitrary radius r is selected artificially from such effective channel and is considered as quasi-uniform in length. Then we can operate with such a characteristic as the magnetic permeability of this thin tube (Sandulyak, 1983, 1984; Sandulyak et al, 2009, 2007). Naturally, tubes of different radius r will be characterized by different permeability $\tilde{\mu}$ (due to a variable thickness of the space between the balls surfaces), which increases as the channel axis is approached and decreases as it moves away from it (Fig. 9.1b). This determines the

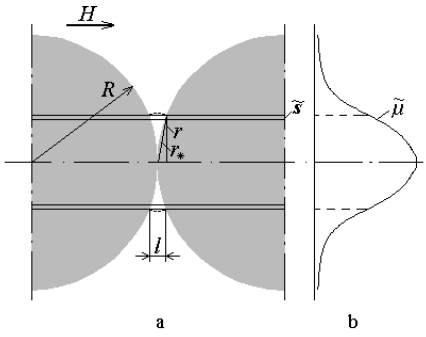

Fig. 9.1 The module (segment) of the chain of the balls with dedicated elementary layered tube of the effective magnetization channel (a) and illustration of the extreme permeability profile (b) of the channel in its cross section (in the radial direction).

[1] Hereinafter we mean the magnetic resistance in its classical definition, i.e. as the ratio of the magnet length to its cross-section and absolute magnetic permeability, but not in the often used, mentioned earlier, interpretation of the "giant magnetoresistance" - as the relative change in the electrical resistivity under magnetic conditions.

presence of a radial, extreme by shape permeability profile $\tilde{\mu}$ (and corresponding induction B) for the effective channel. In this case, according to the mentioned formal analogy with the velocity profile of a fluid flow in a pipe, the analog of velocity here is, of course, magnetic induction (as the magnetic flux per area unit). As for the magnetic permeability - as induction, referred to the product $\mu_0 H$ (where: $\mu_0 = 4\pi 10^{-7}$ H/m - magnetic constant, H - magnetizing field strength), then such a comparison is valid up to a multiplier $1/\mu_0 H$.

The parameters here and hereinafter (in the framework of the channeled magnetization model), namely the average permeability of the layer-tubes of an effective magnetization channel, its cores (and associated average induction in the layer-tubes and core) are amenable to the corresponding experimental determination and theoretical calculation.

9.4 Data of the In-Channel (Core and Layer-Tube) Magnetic Flux, Average Induction, and Permeability

To obtain the necessary information on the magnetization channel and its features one can experimentally use, for example, magnetizable straight chain of balls (Sandulyak, 1983, 1984; Sandulyak et al, 2007, 2009). It should be like any magnet used to study the magnetic properties of its material (in this case quasi-uniform material) sufficiently long, self-sufficient to minimize the demagnetizing factor (as experiments show - with a number of balls not less than 8-10) magnetized in the solenoid with greater length.

Then, using the concentric flow-measuring loops of this or that radius r (section s) placed in the middle of this chain (Fig. 9.2) between adjacent balls of radius R, and micro-webermeter, one can obtain the data of the corresponding magnetic flux Φ through each of these loops (Fig. 9.3). However, because of the limited dimensions of the inter-ball area where the loops are placed from considerations of obtaining data it is advisable to use balls with increased radius also as close as possible to the contact point of the granule-balls, for example, R = 16.65 mm (Sandulyak, 1983, 1984; Sandulyak et al, 2007, 2009).

Measured data Φ are the starting point for calculating the average induction $B = \Phi/s$ in the core of a certain radius r and magnetic permeability $<\tilde{\mu}>= B/\mu_0 H = \Phi/s\mu_0 H$ of this core (Fig. 9.4). The use hereinafter of unusual designation of the

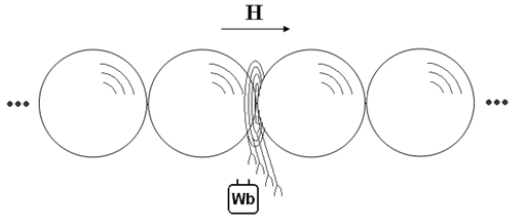

Fig. 9.2 Magnetizable chain of the balls with a system of concentric flow loops located on the plane of symmetry between two central balls.

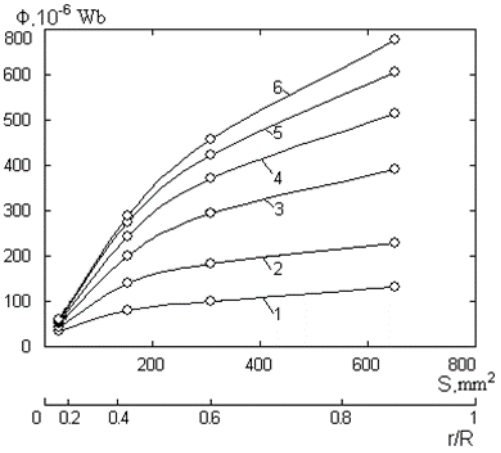

Fig. 9.3 The magnetic flow data obtained through the use of loops in the core of different cross-section (relative radius) of the effective channel of magnetization of the chain of the balls - for different values of the intensity of the magnetizing field H, 1 - H = 18 kA/m, 2 - 36, 3 - 70, 4 - 105, 5 - 140, 6 - 175.

effective magnetization channel quasi-uniform core magnetic permeability, i.e. $<\tilde{\mu}>$, is semantic. It corresponds to the result of averaging of this channel magnetic permeability radial profile $\tilde{\mu}$ within limits of one or another of its cores.

In connection with the obtaining of field dependencies of induction B and permeability $<\tilde{\mu}>$ for various (by radius r and section s) cores (Fig. 9.4, curves 1-4), the field dependencies of induction B and permeability μ_m for granular filling media are of interest (Fig. 9.4, curves 5), as well as the known field dependencies of induction B and permeability μ for a material close to the ball material - low-alloyed steel (Fig. 9.4, curves 6).

The comparison of all these dependencies clearly illustrates the quite expected fact: curves B and $<\tilde{\mu}>$ for the magnetization channel cores as if fill the vast "vacant" area between the curves 6 and 5 for poly-ball medium (Fig. 9.4a) and the curves 6 and 5 for the balls material (Fig. 9.4b). Indeed, as the core radius r (relative to the radius r/R) increases, the induction and permeability curves 1-4 become similar to the corresponding curves 5 for the poly-ball medium, since in this case the core more and more reproduces the effective channel of the poly-ball medium. With decreasing r/R these curves 1-4 approach the corresponding curves 6 for the uniform metal, since for an increasingly thin core the gap between the granules decreases. In this case, in the limit ($r/R \to 0$), a complete concordance of the curves can be expected. In this case, in order to obtain curves 6 in Fig. 9.4 it would be necessary to use (as it is hardly possible) such a control uniform sample that would accurately reproduce the alternation of real untempered and hardened areas (as in balls), or carry out investigations using annealed balls. At the same time, the available known curve for B (Fig. 9.4a, curve 6) is an acceptable approximation to the specific curve of our interest.

Having the field dependencies of induction B and permeability $<\tilde{\mu}>$ for various in-channel cores (Fig. 9.4, curves 1-4), we note a remarkable fact of the decrease in the values of B and $<\tilde{\mu}>$ with an increase in the radius r (relative radius r/R) of the cores. Thus, already here, i.e. at the stage of the corresponding quantitative

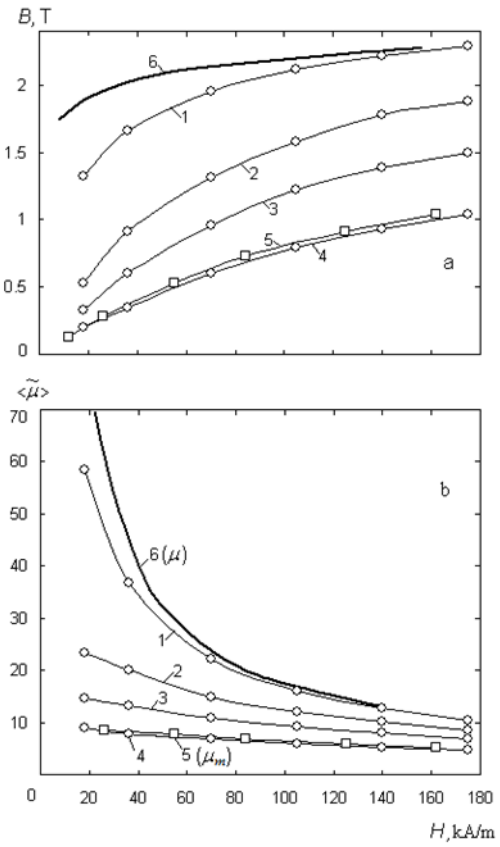

Fig. 9.4 Field dependencies of the average induction (a) in the core of radius r of the effective magnetization channel and average permeability (b) of this core (1 - r/R = 0.17, 2 - 0.42, 3 - 0.59, 4 - 0.87), and here are the corresponding dependencies for the polishing environment (5) and low-alloyed steel (6).

characterization of the cores of the magnetization channel magnetic properties (which deteriorate as they thicken) one can ascertain the existence of the radial profile of this channel magnetic properties. This is illustrated visually (in particular, in coordinates $<\tilde{\mu}>$ vs. r/R) in Fig. 9.5a (points).

In addition, an indicative evidence (even more visually) of the existence of the channel magnetic properties profile is the layer-by-layer (for artificial tubes of this channel) field dependencies B and $\tilde{\mu}$ (Fig. 9.6). They characterize the local (corresponding to a certain radius r of layer-tube) level of effective channel magnetization. To obtain these layer-by-layer field dependencies B and $\tilde{\mu}$ (Fig. 9.6) one need, using the experimental data of magnetic fluxes Φ (Fig. 9.3), just find the difference data $(\Phi_{i+1} - \Phi_i)$ of fluxes between adjacent, i.e. $(i+1)$th and ith concentric loops of radius r_{i+1} and r_i (cross-section s_{i+1} and s_i). On the basis of these data it is easy to obtain the values $B = (\Phi_{i+1} - \Phi_i)/(s_{i+1} - s_i)$, as well as $\tilde{\mu} = B/\mu_0 H$ (hereinafter the previously introduced designation of the layer-tube magnetic permeability is used: $\tilde{\mu}$). Just such local data of induction B and permeability $\tilde{\mu}$ at one or another distance r (relative distance r/R) from the axis of the effective magnetization channel,

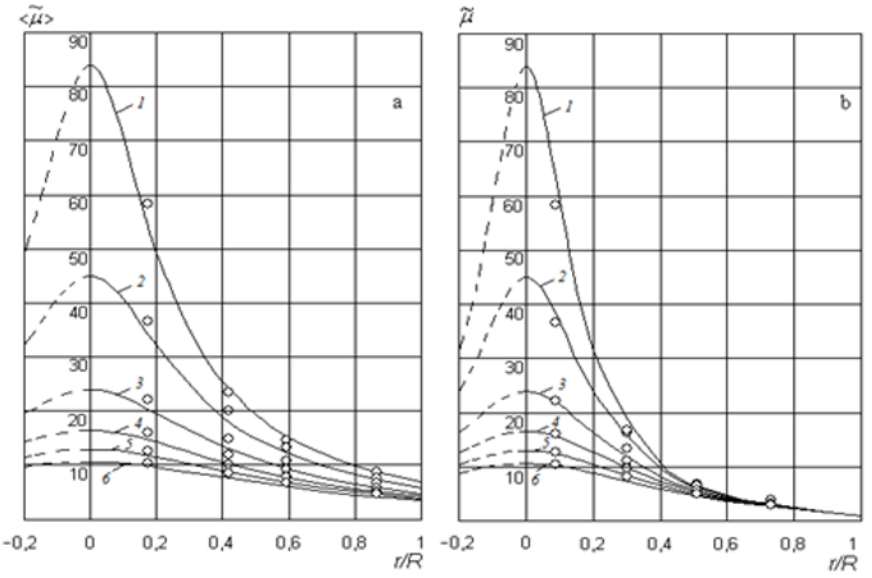

Fig. 9.5: The radial profile of the magnetic permeability of quasi-uniform effective magnetization channel (a) and average permeability of the core (of a certain radius) of this channel (b): 1 - H = 18 kA/m, 2 - 36, 3 - 70, 4 - 105, 5 - 140, 6 - 175; points - experimental data (Figs. 9.4b and 9.6b), lines - calculation from Eqs. (9.1) and (9.5).

as already stated, reflects the very important property of the channel itself - radial profile of its magnetization. In particular, as it indirectly follows from the family of curves B and $\tilde{\mu}$ decomposing by r/R (Fig. 9.6), values B and $\tilde{\mu}$ for the effective magnetization channel decreases with increasing of r/R.

More clearly (in particular, in coordinates $\tilde{\mu}$ of r/R) the radial profile of the magnetic properties of the effective magnetization channel can be traced in Fig. 9.5b (points). In this case, note that despite the formal similarity, here the parameter r/R characterizes not the relative radius of the core-magnet, as it was before, but the average relative radius of the layer-tube of the effective magnetization channel (including the minimum in the experiments of a tube with zero internal radius).

9.5 Magnetizing Channel Layer Tubes: Local Permeability, Radial Profile

To obtain the calculated dependencies characterizing the magnetic properties of quasi-uniform layer-tubes (in particular, their magnetic permeability $\tilde{\mu}$) we first note that in the space between the adjacent balls of the magnetizable chain of balls, especially at

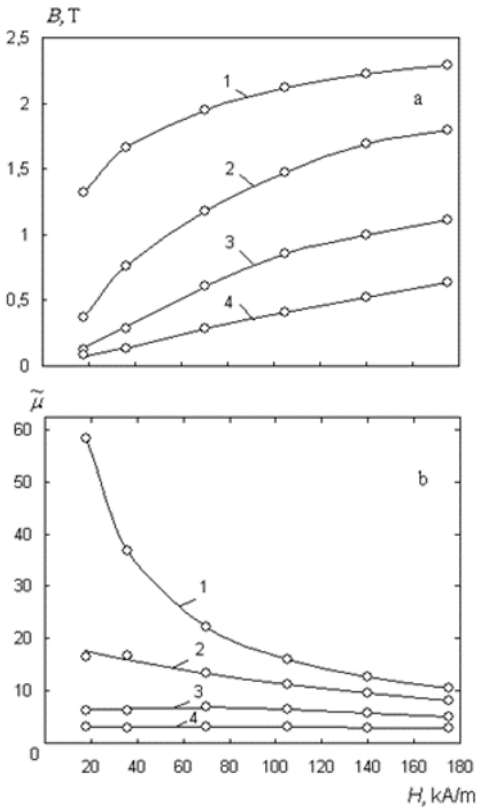

Fig. 9.6 The field dependencies of the average induction (a) in the layer-tube of medium radius r (between the radiuses of the cores, including the smallest core with zero internal radius) of the effective magnetization channel and the average permeability (b) of the tube layer (1 - r/R = 0.09, 2 - 0.3, 3 - 0.51, 4 - 0.73).

elevated values r/R, of course, there is a barrel-like course of magnetic force lines (Fig. 9.1a, dashed lines). In this case, according to the law of their refraction, because of relatively high values of the magnetic permeability of the balls metal these lines emerge from the ball (and enter to the ball) almost normally to its surface. At the same time, the magnetic induction vector, which is tangent to the force line, as it is known, varies not only in direction but also in magnitude. As for the numerical values of induction, at the output of the magnetic force lines from certain ball points located at a distance r from the channel axis (Fig. 9.1a) they practically correspond to the numerical values of induction at the same distance in the middle of the inter-ball space. In this sense the "form" of magnetization channel layer-tubes is actually close to cylindrical. Consequently, if we proceed from this justified simplification (Fig. 9.1a), then the problem of obtaining the calculated dependence for the radial profile of permeability $\tilde{\mu}$ becomes completely solvable (Sandulyak, 1983, 1984; Sandulyak et al, 2007, 2009).

To do this, first, from an infinite set of thin (conditional) concentric layer-tubes of the effective magnetization channel you should select one tube (Fig. 9.1a) with radius r and small cross-section $\tilde{s}$, likening it to such a quasi-uniform (along the length) tube

whose magnetic resistance is equivalent to the total resistance of the corresponding real areas. In this case, the magnetic resistances of a typical link (between adjacent balls centers) of the quasi-uniform tube, section (sections) of the tube in the body of adjacent balls and section of this tube between the balls are, respectively,

$$2R/\mu_0\tilde{\mu}\tilde{s}, \qquad (2R-l)/\mu_0\mu\tilde{s}, \qquad l/\mu_0\tilde{s},$$

where l - tube length between adjacent balls' surfaces (Fig. 9.1a). Secondly, it is necessary to take into account the purely geometrical constraint (Fig. 9.1a):

$$l/2R = 1-[1-(r/R)^2]^{0.5}$$

Then simple transformations of indicated condition for the equivalence of magnetic resistances give an expression reflecting the regularity of the change in the magnetic permeability of quasi-uniform effective magnetization channel in its radial direction

$$\tilde{\mu} = \frac{\mu}{\mu - \sqrt{1-(r/R)^2}(\mu-1)} \tag{9.1}$$

or, in other words, an expression for the radial profile of the channel magnetic permeability.

Figure 9.5b shows the calculated data $\tilde{\mu}$ (lines) obtained by Eq. 9.1, revealing a bell-shaped profile $\tilde{\mu}$ (outwardly similar to the Gaussian normal probability law). It can be seen that these calculated data $\tilde{\mu}$ (lines) are in a good agreement with the experimental data $\tilde{\mu}$ (points), thereby confirming validity of Eq. 9.1 that followed from the model under consideration.

It must also be said that the value l (Fig. 9.1a) for simplicity can also be expressed in terms of the distance r_x from the point of contact of the balls to the point of tube intersection with the ball surface, i.e. $l = r_x^2/R$, and for relatively small r it is often convenient to assume that $r_x \cong r$. Then an alternative to Eq. (9.1), somewhat simplified version of the formula for calculating the radial profile of the magnetic permeability of the effective magnetization channel, will follow:

$$\tilde{\mu} = \frac{\mu}{1+0.5(r/R)^2(\mu-1)} \tag{9.2}$$

Values $\tilde{\mu}$ calculated by Eqs. (9.1) and (9.2) are close, especially when $r/R \le 0.5$ and their difference does not exceed 3-6%.

9.6 Magnetization Channel Core: Average Magnetic Permeability

The calculated dependencies for the average magnetic permeability $<\tilde{\mu}>$ of the core with the arbitrary radius r of the effective magnetization channel can be found by typical averaging for such cases, in this case - by averaging the local (for tube

layers) values of the magnetic permeability $\tilde{\mu}$. In this case we can use two obvious and independent expressions for the magnetic flow through the core:

$$\Phi = \mu_0 < \tilde{\mu} > H\pi r^2, \qquad \Phi = \mu_0 H 2\pi \int_0^r \tilde{\mu} r \mathrm{d}r, \tag{9.3}$$

from which follows necessary expression for the averaging:

$$< \tilde{\mu} >= \frac{2}{r^2} \int_0^r \tilde{\mu} r \mathrm{d}r \tag{9.4}$$

After the corresponding integration, taking into account Eq. (9.1) for $\tilde{\mu}$, follows the formula for the determining of the magnetic permeability $< \tilde{\mu} >$ of the certain core (radius r) of the effective magnetization channel:

$$< \tilde{\mu} >= \frac{2\mu}{(r/R)^2(\mu-1)} \left\{ \frac{\mu}{\mu-1} \ln \left[\mu - (\mu-1) \sqrt{1-\left(\frac{r}{R}\right)^2} \right] + \sqrt{1-\left(\frac{r}{R}\right)^2} - 1 \right\} \tag{9.5}$$

Figure 9.5a shows the calculated data $< \tilde{\mu} >$ (lines) obtained with the use of Eq. (9.5). It can be seen that these data match previously discussed experimental data $< \tilde{\mu} >$ (points), thereby confirming the validity of this calculation Eq. (9.5), which followed from the model considered.

A similar integration can also be performed taking into consideration the simplified Eq. (9.2) for $\tilde{\mu}$, this leads to a simplified formula for $< \tilde{\mu} >$:

$$< \tilde{\mu} > \cong \frac{2\mu}{(r/R)^2(\mu-1)} \ln \left[1 + \frac{1}{2} \left(\frac{r}{R}\right)^2 (\mu-1) \right] \tag{9.6}$$

Values $< \tilde{\mu} >$ calculated in accordance with Eqs. (9.5) and (9.6) are close to each other. For example, for $r/R = 0.5$, they differ by 1-2% and even for $r/R = 1$ - by up to 7-9%. This indicates the possibility of using (where it makes sense) a simpler Eq. (9.6) in a wide range of r/R.

If the values of the magnetic permeability of a metal $\mu \geq 10 - 20$ are really high (as it is seen in Fig. 9.4b), Eq. (9.6) can be even more simplified by taking $\mu \cong (\mu - 1)$, then

$$< \tilde{\mu} > \cong \frac{2\mu}{(r/R)^2} \ln \left[1 + \frac{\mu}{2} \left(\frac{r}{R}\right)^2 \right] \tag{9.7}$$

In this case the values $< \tilde{\mu} >$ calculated by the simplified Eq. (9.7) and the original Eq. (9.5) are sufficiently close to each other; up to the limiting experimental values $r/R = 0.87$ they differ for not more than 3-4%.

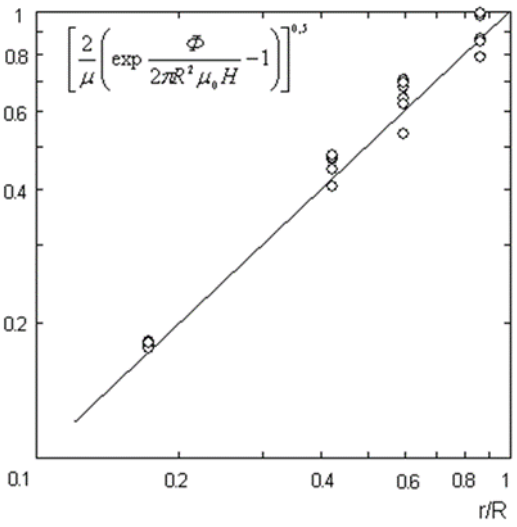

Fig. 9.7 Illustration of the generalization of the data in Fig. 9.3 in the coordinates according to Eq. (9.8).

9.7 Generalized Dependencies for Comparison of the Calculated and Experimental Data

The above-mentioned relevance between calculated and experimental data is witnessing the accuracy of the model, it can be also judged by the generalized (common) dependence. Thus, based on the first of the expressions (9.3) and obtained convenient simplified Eq. (9.7), simplified but still acceptable for the description of all the primary experimental data which is shown in Fig. 9.3, the expression for the magnetic flow Φ in the core of the channel is written. The obtained expression presented later as:

$$\left[\frac{2}{\mu}\left(\exp\frac{\Phi}{2\pi R^2\mu_0 H}-1\right)\right]^{0.5} \cong \frac{r}{R} \tag{9.8}$$

is quite suitable for the generalization of the whole data array.

For the illustration of such generalization (in the form of common dependence) all the numerous primary experimental data of magnetic flows Φ (Fig. 9.3) and other data included in (9.8), such as the radius of the flow-measuring loops r, the radius of balls R, the intensity of the magnetizing field H, magnetic permeability of the material of the balls μ must be processed in the specific coordinates on which the left and right parts of Eq. (9.8) point out. In fact, the coordinates here (dimensionless) are tied to the radius of the flow-measuring loop, as seen by the right side of expression.

Indeed, in such coordinates the experimental and calculated data must obey (and in fact obey, as seen in Fig. 9.7) to the bisectrix of the right angle of this coordinate system, and this fact with such a generalized analysis confirms the validity of the considered model.

Another example of a demonstrative proof of generalization is similar to the previous one and here can be used similar approach, also using the first of Eqs. (9.3) and simplified Eq. (9.7) - to obtain such an expression:

$$\frac{\Phi}{\pi R^2} \cong 2\mu_0 H \ln\left[1 + \frac{\mu}{2}\left(\frac{r}{R}\right)^2\right] \tag{9.9}$$

As seen from the left side of Eq. (9.9), the coordinates of this variant of generalization are tied to some formal induction (as a magnetic flow through a loop with radius r and which is related to the cross section of the ball).

Figure 9.8 shows that in such generalizing coordinates, the experimental and calculated data (here, in contrast to the previous version, in a more dispersed form), too, are expectedly comply with the bisectrix of the right angle of this coordinate system, which one more time confirms the validity of the considered model.

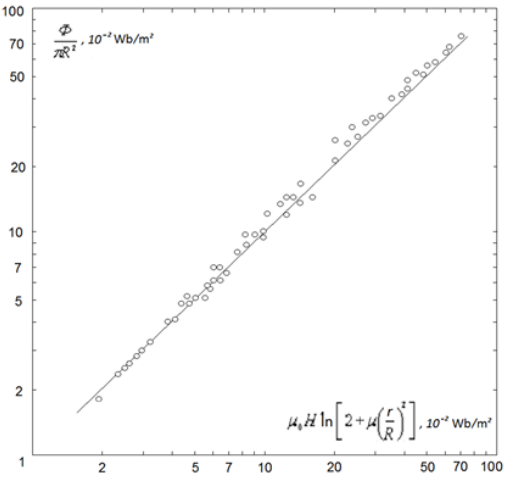

Fig. 9.8 Illustration of the generalization of the data in Fig. 9.3 in the coordinates according to Eq. (9.9).

9.8 Magnetization Channel and Harness of the Channels (in the Ferromaterial Filling): Average Magnetic Permeability

One of the important consequences of Eqs. (9.5)-(9.7) is that they can be used to obtain the values of the magnetic susceptibility $<\tilde{\mu}>$ of the entire effective channel of magnetization (here - the straightened chain of the pellet balls). For this, in (9.5)-(9.7), we only need to take $r/R = 1$, i.e. to use any of these formulas:

$$
\begin{aligned}
&<\tilde{\mu}> = \frac{2\mu}{\mu-1}\left(\frac{\mu}{\mu-1}\ln\mu - 1\right),\\
&<\tilde{\mu}> \cong \frac{2\mu}{\mu-1}\ln\left(\frac{\mu+1}{2}\right),\\
&<\tilde{\mu}> \cong 2\ln\left(1+\frac{\mu}{2}\right)
\end{aligned}
\tag{9.10}
$$

Equations (9.10) can become the basis for obtaining formulas that allow the calculation of the magnetic susceptibility of the dispersed ferromaterial μ_m (filling of granules or grains) - as a harness of the magnetization channels. For this, in Eq. (9.9) the factor 1.44 (Sandulyak et al, 2007) should be used, taking into account the difference (note - up to a constant) of the harness of the branched chain channels (in filling, for example, pellet balls, i.e. in the structure of meandering chains of granules) in the comparison with the analyzed solitary channel here (in the chain of rectified pellet balls). Then the desired formulas will be:

$$
\mu_m = \frac{2.9\mu}{\mu-1}\left(\frac{\mu}{\mu-1}\ln\mu - 1\right), \quad \mu_m \cong \frac{2.9\mu}{\mu-1}\ln\left(\frac{\mu+1}{2}\right), \quad \mu_m \cong 2.9\ln\left(1+\frac{\mu}{2}\right) \tag{9.11}
$$

Consequently, it becomes possible to describe analytically the magnetization curve (B vs. H) of such a material - based on the well-known expression

$$
B = \mu_m \mu_0 H, \tag{9.12}
$$

but with the use of Eq. (9.11) for μ_m. Of course, we must bear in mind that shown in (9.11) and, consequently, in the corresponding ones, written according to (9.12) with respect to (9.11), in formulas for the desired average induction B, the magnetic permeability of the substance of the balls (low-carbon steel) μ has an individual relationship with the intensity of the magnetizing field H. This can be seen, in particular, from curve 6 in Fig. 9.4b, the data of which should be taken into account directly or by means of an additional calculation from the formula:

$$
\mu = (H_\mu / H)^{0.9} \tag{9.13}
$$

on the basis that the field dependencies of the magnetic permeability of steels in the post-extremal region are subject to a power-law coupling of the type (9.13) (Sandulyak et al, 2010, 2015b), up to the parameter H_μ (here $H_\mu = 24.4 \cdot 10^5$ A/m).

The calculated field dependencies of the induction B (magnetization curves of the spherical environment) obtained using Eqs. (9.11) - (9.13) agree with the experimental dependence (Fig. 9.4a, curve 5), which confirms the validity of these (and preceding) calculation formulas that followed from the considered model.

We note that the representation of the scattered formulas (9.11)-(9.13) in the form of one or another desired common expression was not realized here because of the obvious cumbersomeness of this expression. At the same time, it is possible to avoid such defect if in Eqs. (9.11) it is justified (as for the actually high values of μ, as seen in Fig. 9.4b), as before, assume that $(\mu - 1) \cong \mu$, and also $(\mu + 1) \cong \mu$. Then, in

particular, using Eq. (9.12), the first and the second of Eqs. (9.11) and also Eq. (9.13), one can obtain such compact original formulas for calculating the magnetization curve of a granular (grainy) filling environment:

$$B = 2.9\mu_0 H\left(0.9\ln\frac{H_\mu}{H} - 1\right), \qquad B = 2.6\mu_0 H\ln\left(0.46\frac{H_\mu}{H}\right) \tag{9.14}$$

9.9 The Physical Meaning of the Profile Permeability. Relative Field Strength Between Ferroelements

Equations (9.1) and (9.2) for the magnetic permeability of a layer-tube $\tilde{\mu}$ with radius r, as a matter of fact, turn to become passing decisions of one more key problem. Thus, they are formulas for calculating the field strength between ferroelements h (related to the magnetizing, i.e. external field H) at a particular point at a distance r from the point of contact of ferroelements-balls of radius R in the area between them, and more exactly:

$$\frac{h}{H} = \tilde{\mu} = \frac{\mu}{\mu - \sqrt{1-(r/R)^2}(\mu-1)}, \qquad \frac{h}{H} = \tilde{\mu} \cong \frac{\mu}{1+0.5(r/R)^2(\mu-1)} \tag{9.15}$$

This, in particular, follows from the identical expressions for magnetic induction: in the quasi-uniform tube such as $B = \mu_0\tilde{\mu}H$ and in the inter-sphere region as $B = \mu_0 h$.

Actually, the simple expression (relation) obtained here $\tilde{\mu} = h/H$ also reveals the physical meaning of a such parameter, inherent exclusively to the model of channeled magnetization, as a profile (local, characterizing quasi-uniform layer-tubes) magnetic permeability $\tilde{\mu}$. As already noted, the parameter $\tilde{\mu}$ characterizes the relative field strength in the area between the ferroelements (granules, grains).

On the basis of (9.15), it is not difficult to verify (also using the data in Fig. 9.5b) which is located in the vicinity of the point of contact of the ferroelements (up to $r/R = 0.4 - 0.5$): $h \gg H$ (Fig. 9.9a). In this case, the values of the field strength between the ferroelements h can significantly differ (Fig. 9.10a) even at relatively moderate values of the magnetizing (external) field strength H.

Having the calculated Eqs. (9.15), it is not difficult to find the dependencies of the heterogeneity in the area between ferroelements (they are particular necessary for magnetophoresis problems), to be more specific, in the radial direction of the plane of symmetry, i.e. moving away along (by r) from the point of contact of ferroelements (Fig. 9.1a) - as the derivative $\mathrm{d}h/\mathrm{d}r$:

$$\left|\frac{\mathrm{d}h}{\mathrm{d}r}\right|\frac{R}{H} = \frac{\mu(\mu-1)(r/R)}{\sqrt{1-(r/R)^2}\left[\mu - \sqrt{1-(r/R)^2}(\mu-1)\right]^2} \tag{9.16}$$

$$\left|\frac{\mathrm{d}h}{\mathrm{d}r}\right|\frac{R}{H} = \frac{\mu(\mu-1)(r/R)}{\left[1+0.5(r/R)^2(\mu-1)\right]^2} \tag{9.17}$$

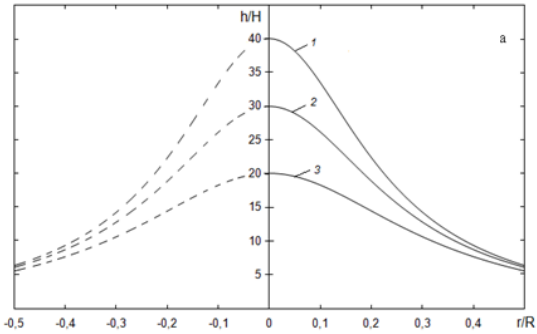

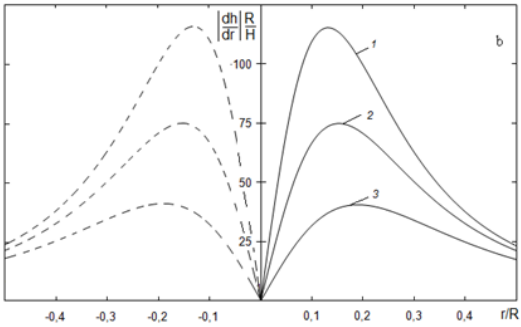

Fig. 9.9 The relative values of the field strength h/H (a) and the heterogeneities $|\mathrm{d}h/\mathrm{d}r|R/H$ (b) between the balls-elements of the chain of balls - as r is moved away from the point of contact of the balls for different magnetic field strength H (magnetic permeability of the metal of the balls μ), 1 - H = 40 kA/m ($\mu \cong 40$), 2 - H = 55 kA/m ($\mu \cong 30$), 3 - H =85 kA/m ($\mu \cong 20$).

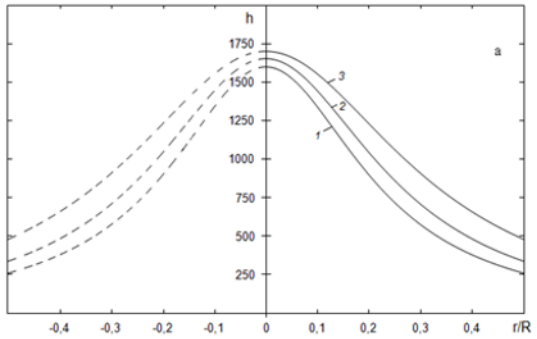

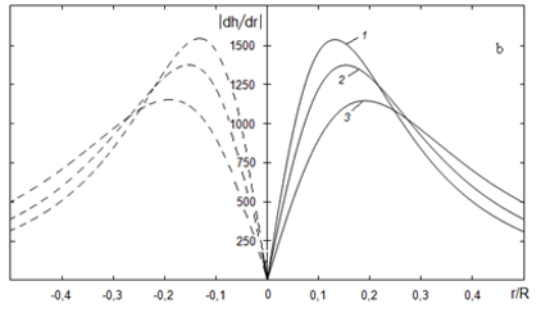

Fig. 9.10 The same as in Fig. 9.9 but for absolute values of the field strength h (a) and heterogeneity $|\mathrm{d}h/\mathrm{d}r|$ (b) - with a radius of ferroelements-balls R = 3 mm.

An illustration of the dependencies (9.16) and (9.17) which indicates their extreme form, is shown in Fig. 9.9b. Moreover, from the simplified formula (9.17), and also using the link (9.13) and assuming, as before $(\mu - 1) \cong \mu$, followed by convenient expressions for the abscissa and the ordinates of the extreme:

$$\left(\frac{r}{R}\right)_{\text{extr}} = \frac{1}{\sqrt{1.5(\mu - 1)}} \cong 0.82\left(\frac{H}{H_\mu}\right)^{0.45}, \tag{9.18}$$

$$\left(\frac{\mathrm{d}h}{\mathrm{d}r}\frac{R}{H}\right)_{\text{extr}} = 0.46\mu\sqrt{\mu - 1} \cong 0.46\left(\frac{H_\mu}{H}\right)^{1.35}, \tag{9.19}$$

Equations (9.15)-(9.19) allow us to obtain important information (and to analyze it) about the field strength and its heterogeneity both in the relative, dimensionless (written here and shown in Fig. 9.9a, b), as well as in dimensional form (Fig. 9.10a, b). In the latter case, i.e. at the corresponding values of the characteristic dimensions of the ferroelements, in particular, the radius R of the pellet balls (Fig. 9.10a, b), the user receives an additional amount of necessary information: about the actual current values of the field strength and its heterogeneity, about the individual values of the ordinates and abscissas of the extremal values of heterogeneity, the width of the bands in the area of extremes, etc.

9.10 Conclusions

An attempt has been made to classify heterogenous, disperse ferromaterials based on the characteristic values of the volume fraction of the ferrocomponent γ. An estimate was made for the three expressed (especially from the position of the behavior of the demagnetizing factor of the "short" sample of such material) intervals of γ. In this case, such classification is due to the corresponding location of the ferroelements (including contact-less and contact), on which the degree of their mutual magnetic influence depends.

It has been established that materials in the form of fillings of ferroelements (granules, grains), as a widespread class of such ferromaterials, are characterized by practically constant value of $\gamma \cong 0,6$. These materials are of independent interest for research, in particular, for the purpose of determining the averaged magnetic properties (magnetic permeability, induction) and obtaining information (especially important in the field of filtering magnetophoresis) about the field between ferroelements.

Conceptually and in details (on the example of a chain of contacting balls) the productive model of the channeled magnetization of these "tightly packed" ferromaterials is stated. It allows us to establish analytical expressions and calculated dependencies (consistent with the experimental data) for the average magnetic permeability of the magnetization channel and its parts (cores, tube layers of different radius r), and also dispersed ferromaterial as a whole (as a "harness" of branched

channels). The compliance of the results of the experiments and calculations is also illustrated in the form of generalizing dependencies.

It is shown that in the physical sense the magnetic permeability of a layer-tube with radius r of the magnetization channel characterizes the relative (related to the intensity of the magnetizing field) field strength between contacting ferroelements (for example, balls) at a distance r from their point of contact. This also makes it possible to obtain expressions characterizing the heterogeneity of the field between ferroelements.

Acknowledgements The research is conducted with financial support from RFFI within the frameworks of research project No 16-38-60034 mol_a_dk and from Russian Federation Ministry of Education and Science No 9.9626.2017.

References

Anhalt M, Weidenfeller B (2007) Magnetic properties of polymer bonded soft magnetic particles for various filler fractions. Journal of Applied Physics 101(2):023,907

Anhalt M, Weidenfeller B, Mattei JL (2008) Inner demagnetization factor in polymer-bonded soft magnetic composites. Journal of Magnetism and Magnetic Materials 320(20):e844 – e848

Bennacer L, Ahfir ND, Bouanani A, Alem A, Wang H (2013) Suspended particles transport and deposition in saturated granular porous medium: Particle size effects. Transport in Porous Media 100(3):377–392

Bottauscio O, Chiampi M, Manzin A (2009) Homogenized magnetic properties of heterogeneous anisotropic structures including nonlinear media. IEEE Transactions on Magnetics 45(10):3946–3949

Daniel L, Corcolle R (2007) A note on the effective magnetic permeability of polycrystals. IEEE Transactions on Magnetics 43(7):3153–3158

Diguet G, Beaugnon E, Cavaillé J (2010) Shape effect in the magnetostriction of ferromagnetic composite. Journal of Magnetism and Magnetic Materials 322(21):3337–3341

Hultgren A, Tanase M, Felton EJ, Bhadriraju K, Salem AK, Chen CS, Reich DH (2005) Optimization of yield in magnetic cell separations using nickel nanowires of different lengths. Biotechnol Prog 21:509–515

Kim YS, Whittle AJ (2006) Filtration in a porous granular medium: 2. application of bubble model to 1-d column experiments. Transport in Porous Media 65(2):309–335

Lacoste D, Lubensky TC (2001) Phase transitions in a ferrofluid at magnetic-field-induced microphase separation. Physical Review E 64:041,506–1–041,506–8

Mattei JL, Floc'h ML (2003) Percolative behaviour and demagnetizing effects in disordered heterostructures. J Magnetism Magnetic Mater 257(2-3):335 – 345

Ngo AT, Pileni MP (2001) Assemblies of ferrite nanocrystals: Partial orientation of the easy magnetic axes. The Journal of Physical Chemistry B 105(1):53–58

Nielsch K, Wehrspohn RB, Barthel J, Kirschner J, Fischer SF, Kronmüller H, Schweinböck T, Weiss D, Gösele U (2002) High density hexagonal nickel nanowire array. Journal of Magnetism and Magnetic Materials 249(1):234–240

Ravnik J, Hriberšek M (2013) High gradient magnetic particle separation in viscous flows by 3D BEM. Computational Mechanics 51(4):465–474

Sandulyak A, Sandulyak A, Ershova V, Polismakova M, Sandulyak D (2017a) Use of the magnetic test-filter for magnetic control of ferroimpurities of fuels, oils, and other liquids (phenomenological and physical models). Journal of Magnetism and Magnetic Materials 426:714–720

Sandulyak AA, Ershova VA, Ershov DV, Sandulyak AA (2010) On the properties of short granular magnets with unordered granule chains: a field between the granules. Solid State Physics 52(10):2108–2115

Sandulyak AA, Sandulyak DA, Ershova VA, Kiselev DO, Sandulyak AV (2015a) Finding out the commonalities in functional expressions for demagnetizing factor of quasi-solid and solid magnets. In: Proceedings of the World Congress on Engineering 2015, WCE 2015, London, UK, Lecture Notes in Engineering and Computer Science, vol II, pp 1183–1185

Sandulyak AA, Ershova VA, Sandulyak DA, Sandulyak AV, Polismakova MN, Kiselev VA (2016a) Modeling of tubular pores in free-flowing bulk media on the basis of quasi-facetted cells of such media. Glass and Ceramics 73(5):190–192

Sandulyak AA, Polismakova MN, Sandulyak AV, Sandulyak DA, Khlustikov DS (2016b) Model of quasifaceted cells and possibility of its application to free-flowing materials. Glass and Ceramics 72(11):420–424

Sandulyak AA, Ershova VA, Sandulyak DA, Sandulyak AV, Polismakova MN (2017b) Fills of co-sized and different-sized granules as quasi-ordered structures. Journal of Engineering Physics and Thermophysics 90(2):329–335

Sandulyak AA, Polismakova MN, Kiselev DO, A SD, Sandulyak AV (2017c) On limiting the volume fraction of particles in the disperse sample (for the tasks on controlling their magnetic properties). Fine Chemical Technologies 12(3):58–64

Sandulyak AV (1982) Model' namagnichivaniya poristoy sredy (magnetization model of porous media, in Russ.). Technical Physics 52(11):2267–2269

Sandulyak AV (1983) Physicheskaya model' osagdeniya ferromagnitnykh chastiz v namagnichennoy granulirovannoy srede (physical model of sedimentation of ferrous particles in granulated media, in Russ.). Doklady Akademii nauk UkrSSR (9, iss. B):49–53

Sandulyak AV (1984) Namagnichivaniye zepochki sharov (magnetization of the balls chain, in Russ.). Technical Electrodynamics (5):102–104

Sandulyak AV, Sandulyak AA, Ershova VA (2007) Magnetization curve of a granulated medium in terms of the channel-by-channel magnetization model (new approach). Doklady Physics 52(4):179–181

Sandulyak AV, Sandulyak AA, Ershova VA (2008) Functional correction to the classical expression for the average flow velocity in a closely packed granular bed. Theoretical Foundations of Chemical Engineering 42(2):220–224

Sandulyak AV, Sandulyak AA, Ershova VA (2009) On the model of channel-by-channel magnetization of a granular medium (with a radial permeability profile of a quasi-continuous channel). Technical Physics 54(5):743–745

Sandulyak DA, Sandulyak AA, Kiselev DO (2015b) Granular ferromagnets: Formulas for effective magnetic permeability. In: Proceedings of International Conference on Materials Engineering and Industrial Applications, Hong Kong, pp 261–266

Sandulyak DA, Sleptsov VV, Sandulyak AA, Sandulyak AV, Ershova VA, Doroshenko AV (2015c) Filtration magnetophoresis process: an approach to choosing a speed regime. In: Rudas IJ (ed) Proceedings of the 2015 International Conference on *Recent Advances in Mechanics, Mechatronics and Civil, Chemical and Industrial Engineering*, Zakynthos Island, Greece, pp 72–76

Sandulyak DA, Sandulyak AA, Ershova VA, Sandulyak AV, Kononov MA (2017d) Definition of pore tortuosity in granular medium ply based on model of quasi-faceted cells and pore-tubes. Glass and Ceramics 73(9):338–341

Schulz L, Schirmacher W, Omran A, Shah SV, Böni P, Petry W, Müller-Buschbaum P (2010) Elastic torsion effects in magnetic nanoparticle diblock-copolymer structures. J Phys: Condens Matter 22:346,008

Zhang DZ, M RR (2003) Effects of long and short relaxation times of particle interactions in dense and slow granular flows. In: Proc. of ASME FEDSM' 03, 4th ASME_JSME Joint Fluids Engineering Conference, Honolulu, Hawaii, USA, vol 1, pp 579–582